PROCEEDINGS, Thirty-Sixth Workshop on Geothermal Reservoir Engineering
Stanford University, Stanford, California, January 31 - February 2, 2011
SGP-TR-191

# EFFECT OF NATURAL CONVECTION PATTERNS ON OPTIMAL LOCATION AND SIZE OF A HEAT SINK IN A GEOTHERMAL RESERVOIR

Y. Feng, M. Tyagi and C.D. White

Louisiana State University
Baton Rouge, LA, 70802, USA
E-mail: yfeng1@tigers.lsu.edu

## ABSTRACT

Geothermal energy resources such as geopressured geothermal brine (GGB) reservoirs and hot saline aquifers (HSA) can be potential clean energy resources provided the heat extraction from the subsurface is done in an economic and environmental friendly manner. In the proposed study, we are simulating the heat transfer processes around a downhole heat exchanger placed in a long lateral wellbore in a confined geothermal reservoir. Natural convection patterns in saturated porous media that are induced due to the heat extraction process influence the overall amount of heat extracted. Verification and validation studies are presented to evaluate the predictive capability of a thermal reservoir simulator. Several parametric studies (15 cases) are presented to quantify the role of the natural convection on the optimal location and the length of the downhole heat exchanger (DHE).

## INTRODUCTION

During the geothermal heat extraction process, the fluid flow in the porous media could control the heat transport rate both by natural convection as well as forced convection. The role of natural convection is typically small as compared to the forced convection and depends on reservoir geometry as well as properties. However, at the time scales of long production life of the geothermal resource, natural convection could play a significant role. For geothermal resources such as GGB and HAS, natural convection may be significant during and after heat extraction to impact the overall heat extracted.

The present simulation study focuses on the fluid flow and heat transfer processes around a DHE placed in a long lateral wellbore in a confined saturated geothermal reservoir. The DHE is represented as a horizontal heat sink with linearly varying specified temperature located in the saturated aquifer layer. Several parametric cases are studied to include the effect of DHE length and its vertical position on the heat transfer rate as well overall heat extracted.

## NATURAL CONVECTION SIMULATION IN A GEOTHERMAL RESERVOIR

### Natural Convection

Natural convection is the fluid motion generated by density differences due to temperature gradients. The ratio of the natural convection to the conduction is given by a dimensionless group, Rayleigh number (Eq. 1).

$$Ra = \frac{\rho_f g \beta x^3 (\Delta T)}{\mu \alpha_m} \quad (1)$$

where,

$$\alpha_m = \frac{k_m}{(\rho c_p)_f} \quad (2)$$

In porous media, the Rayleigh number expression also accounts for the medium permeability (Eq. 3), and is also known as the Rayleigh-Darcy number.

$$Ra_D = \frac{\rho_f g \beta K x \Delta T}{\mu \alpha_m} \quad (3)$$

x: characteristic length
g: gravity acceleration
ΔT: temperature difference
μ: dynamic viscosity
ρ: density
α: thermal diffusivity
β: thermal expansion coefficient
K: permeability
$c_p$: specific heat capacity
k: thermal conductivity

**Heat Transfer in Porous Media**

Neglecting radiative effects and viscous dissipation, the governing equation for the thermal energy transport is given as follows (Eq. 4).

$$(\rho c)_m \frac{\partial T}{\partial t} + (\rho c_p)_f v \cdot \nabla T = \nabla \cdot (k_m \nabla T) + q'''_m \quad (4)$$

where,

$$(\rho c)_m = (1-\varphi)(\rho c)_s + \varphi(\rho c)_f \quad (5)$$

$$k_m = (1-\varphi)k_s + \varphi k_f \quad (6)$$

$$q'''_m = (1-\varphi)q'''_s + \varphi q'''_f \quad (7)$$

Thermal transport is solved using finite difference method coupled with Darcy's law and continuity equation for velocity field calculation.

The following equations indicate the correlations between fluid density vs. temperature and pressure, where, $\beta$ and $C$ represents thermal expansion coefficient and compressibility, respectively.

$$\rho_f = \rho_{ref}\left[1 - \beta\left(T - T_{ref}\right)\right] \quad (8)$$

$$\rho_f = \rho_{ref}\left[1 + C\left(P - P_{ref}\right)\right] \quad (9)$$

**Thermal Circuit around DHE**

Temperature boundary conditions around a heat sink can be studied using a thermal circuit. Thermal resistance is defined as the temperature difference across a structure when a unit of heat energy flows through it in unit time. The heat transfer between DHE and its surrounding gridblocks is dominated by both conduction and natural convection. The thermal circuit can be illustrated by Figure 1, from which, the overall thermal resistivity can be expressed as Eq. (10).

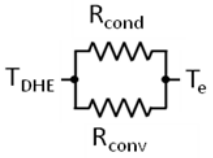


*Figure 1: Thermal circuit around DHE.*

$$R_{overall} = \frac{1}{\frac{1}{R_{conv}} + \frac{1}{R_{cond}}} \quad (10)$$

The following two equations indicate the thermal resistivities for both conduction and convection (Bauer, 2010).

$$R_{cond} = \frac{1}{2\pi k_m} ln\left(\frac{d_e}{d_{DHE}}\right) \quad (11)$$

$$R_{conv} = \frac{1}{Nuk_f\pi}\frac{d_e - d_{DHE}}{d_{DHE}} \quad (12)$$

where, Nu is Nusselt number (the ratio of convective to conductive heat transfer coefficient) and $d_e$ is the effective diameter. Merkin (1978) studied the problem of a horizontal cylinder embedded in porous media and provided following correlation.

$$Nu = 0.565 Ra_D{}^{0.5} \quad (13)$$

**Verification &Validation Tests**

The following two cases from published literature are compared against the simulation results for corresponding parameters and boundary conditions.

***Case I (Costa, 2006):***

In the first case, left boundary is maintained at a high temperature and right boundary at a low temperature (Figure 2). Top and bottom boundaries are insulated. Figure 3 presents the results on temperature profile (left) and velocity field (right) for $Ra_D$=100. Comparison of the isotherms as well as streamline between our results and Costa's results is satisfactory.

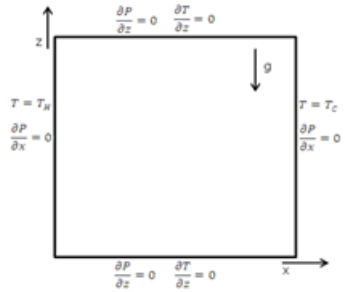


*Figure 2: Boundary conditions for Case I.*

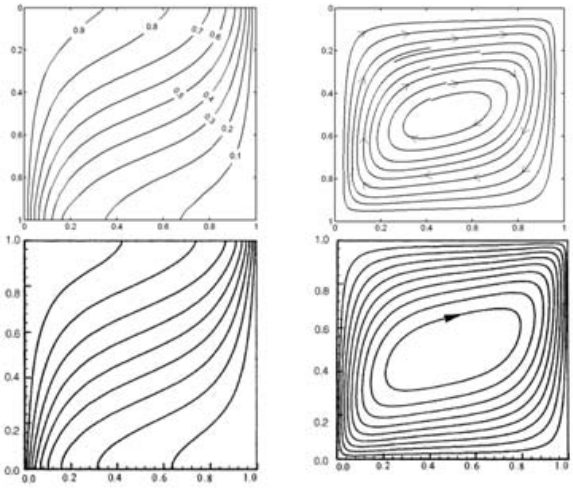

*Figure 3: Comparison of isotherms (left) and streamline (right) [Top row: Present work; Bottom row: Costa (2003, 2006)].*

***Case II (Sathiyamoorthy et al. 2007):***

In the second case, the bottom wall is uniformly heated with constant temperature, right wall is maintained at cold temperature, top wall is adiabatic and the left wall is linearly heated (Figure 4). Figure 5 displays the comparison of present work with Sathiyamoorthy et al. (2007) on isothermal contours for $Ra_D$=100.

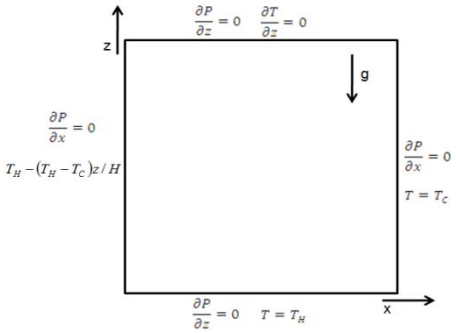


*Figure 4: Boundary condition for Case II.*

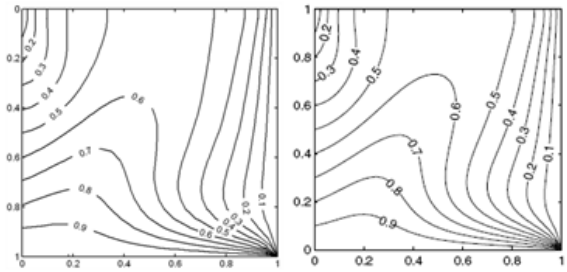

*Figure 5: Comparisons of isotherm contours from present work (left) and Sathiyamoorthy, 2007 (right).*

## RESULTS

### Natural Convection around DHE in GGB

Flow in a simple homogenous geothermal reservoir model with constant properties is presented to assess the natural convection effects on the heat extraction (Figure 6).

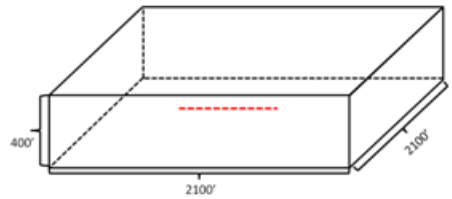


(a)

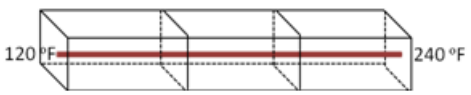


(b)

*Figure 6: (a) Dimensions of geothermal reservoir model; (b) Temperature B.C. around DHE.*

The downhole heat exchanger (DHE) is represented as a heat sink with linear temperature distribution (from 120 $^oF$ at one end to 240 $^oF$ at the other end) located at the center of the confined reservoir along the lateral and transverse directions. The vertical location as well as the length of DHE is varied to study different natural convection patterns generated during the heat extraction process. All six faces of the reservoir are subjected to impermeable flow boundaries. Temperatures at top and bottom are based on a vertical geothermal gradient and no heat flux is specified at the other four faces.

Parameters are used for all simulations are listed in Table 1. The depth of top surface is assumed to be at 11000 ft. The surface temperature is assumed to be 80 $^oF$ with a vertical geothermal gradient of 2 $^oF$/100ft and thus temperature at the top surface is calculated to be 300 $^oF$. Both top and bottom surfaces are maintained under constant heat flux corresponding to this geothermal gradient.

*Table 1: Parameters values used in the simulations.*

| | |
|---|---|
| Viscosity (cp) | 0.15 |
| Fluid density @ [14.7 psia, 100 $^oF$] | 62 |
| Rock density (lbm/ft$^3$) | 168 |
| Rock specific heat capacity (BTU/lbm-$^oF$) | 0.2 |
| Fluid specific heat capacity (BTU/lbm-$^oF$) | 1 |
| Rock thermal conductivity (BTU/ft-day-$^oF$) | 30 |
| Fluid thermal conductivity (BTU/ft-day-$^oF$) | 5 |
| Thermal expansion coefficient ($^oF^{-1}$) | 0.0006 |

Various parametric studies with different vertical placement locations of DHE ($D_H$) {0.05, 0.25, 0.55, 0.75 and 0.95} and its lengths ($D_L$) {0.2, 0.333 and 0.467} are simulated to achieve maximum heat extraction rate for a given temperature distribution.

### Isotherms

Figure 7 shows temperature contours on the x-z plane at y/$L_y$=0.5 for the select cases after 2000 days and 8000 days.

The asymmetric contours are the result of linearly varying temperature along DHE. For a given vertical DHE location, the differences between isotherms

results from the changes in the heat transport around different length DHEs (hence different drainage areas).

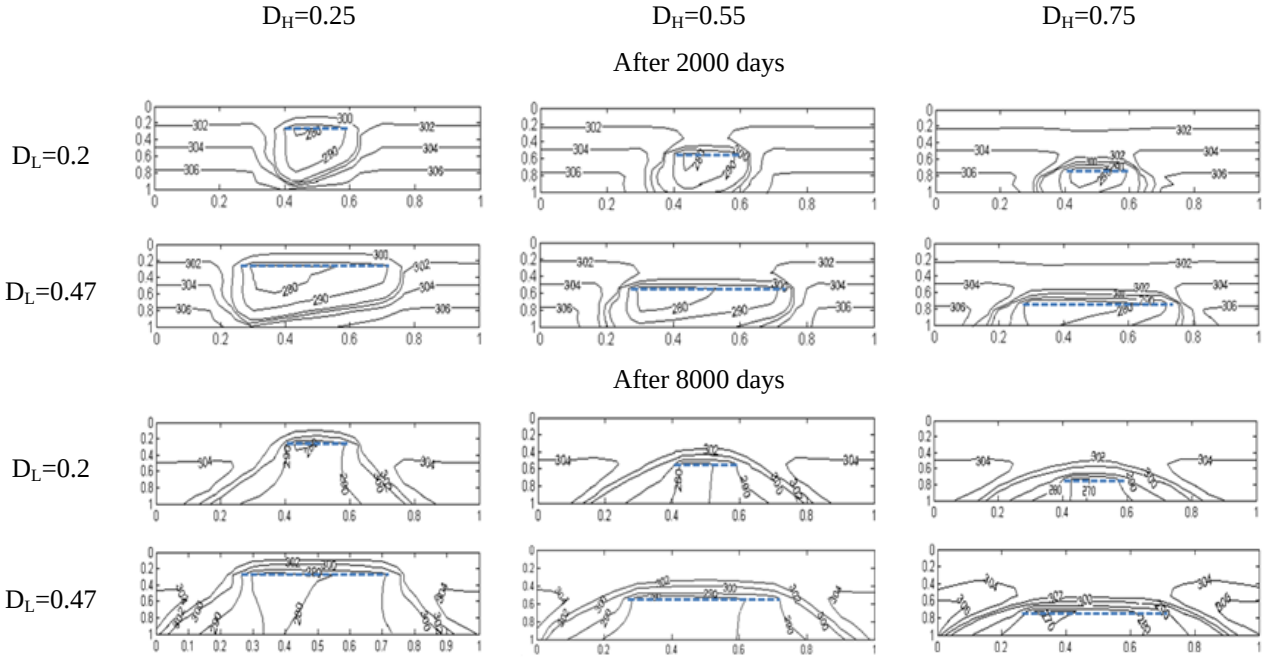


Figure 7: Contour plots of temperature field with $D_H$= {0.25, 0.55 and 0.75} and $D_L$= {0.2 and 0.47} at 2000 days and 8000 days.

At later times (8000 days), the temperature gradients are much larger below the DHE as compared to the shallower depths irrespective of the vertical locations. From the case with $D_H$=0.75, one can see that the large temperature gradients are confined near the reservoir bottom while the top part has only vertical geothermal gradient.

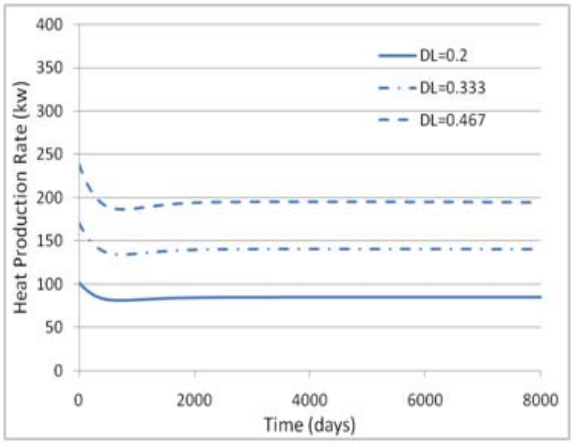


**Heat Extraction Rate and Cumulative Production**

Figure 8 shows that the heat production rate increases with increasing DHE length at a fixed height.

For the very deep DHEs, the heat production rate is declining even after 8000 days. However, for shallower DHEs, the production rate reaches a steady state after the initial transient. Further, the heat production rates are higher shallower DHEs and increasing DHE length contributes more for the shallower DHEs.

It can be argued that deeper DHE could have higher heat production rate initially due to geothermal gradients (higher temperature at deeper zone). However, natural convection effects must contribute significantly in the heat production for shallower DHEs to offset the drawback of lower temperature difference between shallower zone and DHEs.

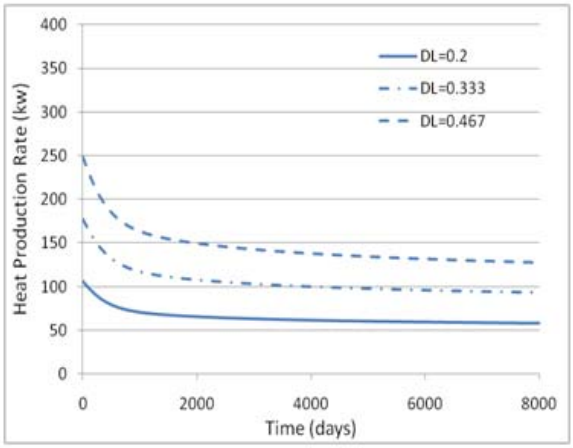


*Figure 8: Heat production rate with $D_H$=0.25(top) and 0.95 (bottom).*

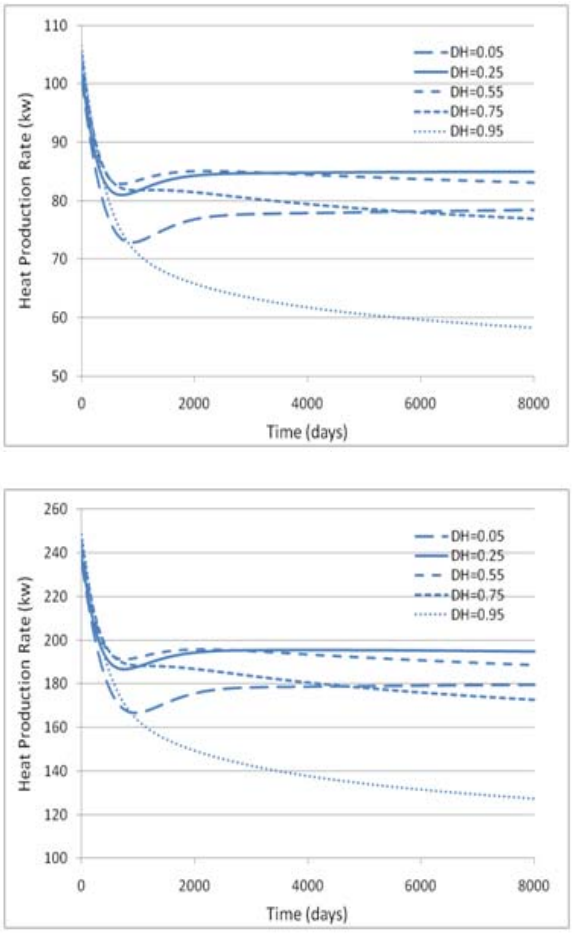


*Figure 9: Heat production rate with $D_L$=0.2(top) and 0.47 (bottom).*

Figure 9 shows that DHE located at vertical depth of $D_H$=0.55 has the highest heat production rate at 3000 days. If the designed production time is as short as 500 days, $D_H$=0.75 would be the best choose. However, if the period extends to 8000 days, the DHE should be setup at $D_H$=0.25.

For long-term development consideration, shallower DHE presents its advantage completely. Even after 20 years production, the heat extraction rate remains steady without observable decline compared to the deeper DHE scenarios considered.

**Optimal Vertical Location**

As noticed in Figure 9, DHE at shallow vertical location may not be the best strategy. When DHE vertical location is near the top boundary of the reservoir ($D_H$=0.05), a significant drop in heat extraction rate is observed during the first 1000 days and this drop is not compensated by any contributions due to natural convection induced heat flux even in a long time durations. Figure 10 shows that the optimal vertical location exists and changes over the operation time.

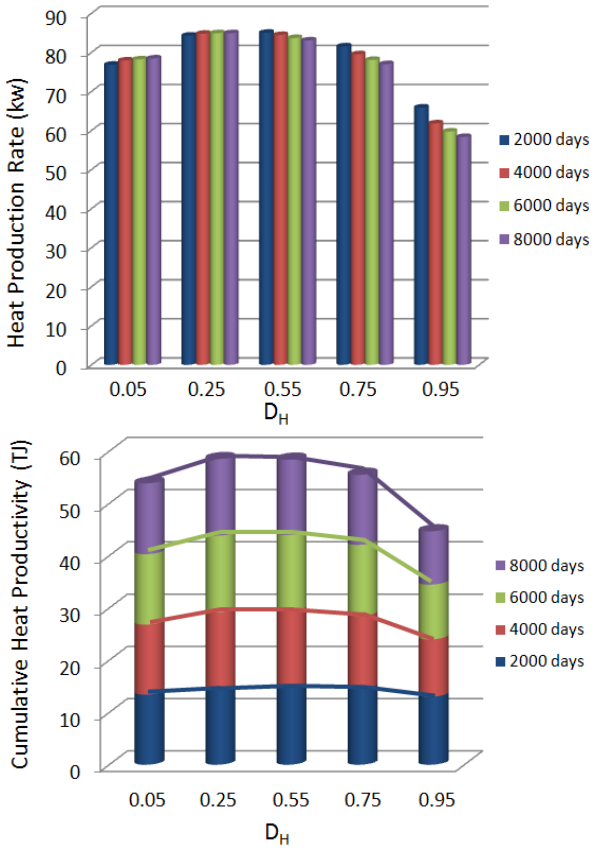


*Figure 10: Heat production rate (top)/Cumulative heat productivity (bottom) vs. locations with $D_L$=0.2 (1TJ=$10^{12}$J).*

Table 2 presents the relationship between optimal dimensionless vertical location and the designed production period for heat production rate and

cumulative productivity for two different dimensionless DHE lengths.

*Table 2: Optimal vertical location vs. designed production time for different DHE lengths.*

| Total Time (days) | Heat Production Rate (kw) | | Cumulative Heat Productivity (TJ) | |
|---|---|---|---|---|
| | $D_L$=0.2 | $D_L$=0.47 | $D_L$=0.2 | $D_L$=0.47 |
| 2000 | 0.439 | 0.419 | 0.56 | 0.544 |
| 4000 | 0.368 | 0.349 | 0.453 | 0.428 |
| 6000 | 0.331 | 0.314 | 0.402 | 0.381 |
| 8000 | 0.311 | 0.296 | 0.373 | 0.354 |

Note that the optimal vertical location of DHE is deeper if maximizing cumulative heat productivity (integral of the heat extraction rates over the designed production time) instead of maximizing the heat production rates.

## CONCLUSIONS

On the basis of several parametric simulation results of natural convection around a linear temperature variation DHE in a confined GGB, following conclusions can be drawn:

- For given vertical location, longer DHE can influence large areas of thermal gradient resulting in enhanced heat extraction rate. However, longer DHE would also require increased capital investment.

- Compared to the shallower DHE which produces heat from the whole reservoir, deeper DHE influences the thermal gradients near the bottom zone in the reservoir only.

- Designed production life is also a critical factor for determining optimal vertical location of DHE. For period less than 10 years, DHE should be located at middle. For long-term (about 20 year), shallower DHE is desired.

- For a given DHE length, the optimal vertical location for maximum heat extraction rate is shallower than that for the maximum cumulative heat productivity.

- Optimal vertical location becomes shallower for both heat production rate and accumulative productivity with increasing DHE length.

## ACKNOWLEDGMENTS

First author (Y. Feng) was supported on a BoR-DOE grant (UcoMS project) during the initial phase of geothermal reservoir simulator development. Computational resources provided by the Center for Computation & Technology (CCT) and The Craft & Hawkins department of petroleum engineering are also gratefully acknowledged.

## REFERENCES

Ahmed, T. 2000, Reservoir Engineering Handbook, second edition. Houston: Gulf Publishing Company.

Aziz, K. and Settari, A. 1979, Petroleum Reservoir Simulation. Society of Petroleum Engineers.

Bauer, D., Heidemann, W., Muller-Steinhagen, H. and Diersch H. J. G. (2010), "Thermal Resistance and Capacity Models for Borehole Heat Exchangers," International Journal of Energy Research, DOI: 10.1002/er. 1689.

Bebout D. G. and Gutierrez D. R.: (1981), "Geopressured Geothermal Resource in Texas and Louisiana - Geological Constraints," Proceedings of the 5th Geopressured-Geothermal Energy Conference held in Baton Rouge, LA.

Chen, Z. 2007, Reservoir Simulation: Mathematical Techniques in Oil Recovery. Philadelphia: Society for Industrial and Applied Mathematics.

Costa, M. L. M., Sampaio, R. and Gama, R. M. S.: (1994), "Modeling and Simulation of Natural Convection Flow in a Saturated Porous Cavity," Meccanica Vol. 29.

Costa, V. A. F. (2003), "Unified streamline, heatline and massline methods for the visualization of two-dimensional heat and mass transfer in anisotropic media," International Journal of Heat and Mass Trans., **46**, 1309-1320.

Costa, V. A. F. (2006), "Bejan's heatlines and masslines for convection visualization and analysis," Appl. Mech. Rev., **59**, 126-145.

Dake, L. P. 1979, Fundamentals of Reservoir Engineering. Amsterdam: Elsevier Science.

Dalal, A. and Das, M. K.: (2008), "Heatline method for the visualization of natural convection in a complicated cavity," International Journal of Heat and Mass Trans. **51**, 263-272.

Hasan, A. R. and Kabir, C. S. 2002, Fluid Flow and Heat Transfer in Wellbores. Richardson, Texas: Society of Petroleum Engineers.

Horne, Roland. (1975), "Transient Effects in Geothermal Convective Systems," A thesis

submitted for PHD at the University of Auckland.

Incropera, F. P. and DeWitt, D. P. 1996, Fundamentals of Heat and Mass Transfer, fourth edition. John Wiley & Sons, Inc.

Merkin, J. H. (1978), “Free Convection Boundary Layers in a Saturated Porous Medium with Lateral Mass Flux,” International Journal of Heat and Mass Trans., **21**, 1499-1504.

Nield, D. A. and Bejan, A. 1998, Convection in Porous media, second edition. New York: Springer Inc.

Patankar, S. V. 1980, Numerical Heat Transfer and Fluid Flow. New York: Hemisphere Publishing Corporation.

Sathiyamoorthy, M., Basak, T., Roy, S. and Pop, I. (2007), “Steady natural convection flow in a square cavity filled with a porous medium for linearly heated side wall(s),” International Journal of Heat and Mass Trans., **50**, 1892-1901.

Vafai, Kambiz. 2000, Handbook of Porous Media. New York: Marcel Dekker Inc.

Wys, N. J. and Dorfman, M.: (1990), “The Geopreshred-Geothermal Resource: Transition to Commercialization,” Proceedings of Industrial Consortium for the Utilization of the Geopressured-Geothermal Resource, EG & G Idaho Inc., Idaho National Engineering Laboratory, p. 9-17